FIELD OBSERVATIONS AND NUMERICAL STUDIES OF HORIZONTAL STRESS EFFECTS ON ROOF STABILITY IN U.S. LIMESTONE MINES

G. S. Esterhuizen
D. R. Dolinar
A. T. Iannacchione
National Institute for Occupational Safety and Health

Abstract

Limestone formations in the United States can be subject to relatively high horizontal stresses owing to the existence of tectonic loading of the limestone strata. Underground limestone mines use the room-and-pillar method, in which 12- to 18-m-wide rooms are typically excavated. The stability of these excavations can be compromised by the horizontal stress, resulting in a rock fall hazard. Rock falls are the cause of 15% of all reportable injuries in underground limestone mines. Horizontal stress related damage can occur in the form of guttering along one or more sides of an excavation, roof beam buckling or oval shaped roof falls, with the long axis perpendicular to the major horizontal stress. Numerical analyses show that the pillar layout and orientation of the mine workings has an effect on the horizontal stress distribution within the roof. The effects of high horizontal stresses can be mitigated by orienting the heading development direction parallel to the maximum horizontal stress, reducing the number of cross-cuts and off-setting the cross-cuts to limit the potential lateral extent of horizontal stress related roof falls. The modeling approach described in this paper can be used as a tool to evaluate potential roof failure and optimize the stability of room and pillar layouts.

1.1 Introduction

The room-and-pillar method of mining is used to recover flat lying limestone deposits in the Eastern and Midwestern United States. The production excavations are 12 to 18 m wide to allow efficient operation of the large underground production equipment. The rooms are typically about 8 m high on initial development and the floor is bench mined in about 30% of the operations to produce a typical final excavation height of about 15 m. The stability of these relatively wide and high excavations must be assured to provide a safe and productive work environment. Fall of ground injuries account for about 15% of lost work days in underground limestone mines [1]. Owing to the large excavation dimensions and the height of the workings, falls of ground can have a devastating effect when they occur.

Horizontal stresses have long been recognized as a source of excavation instability in underground coal and hard rock mines. Hasenfus [2] summarized the historical development of an understanding of horizontal stress issues and mitigation techniques in coal mines, dating back to the 1950's. In hard rock mines horizontal stress induced stability problems have been identified and documented since the 1960's [3, 4].

Horizontal stress related stability issues in U.S. limestone mines and techniques to improve stability by support and changes in mine layout have been well documented in the literature [5, 6, 7, 8, 9, 10, 11]. This paper provides a review of the horizontal stresses and related roof stability issues in U.S. limestone mines, and presents the results of recent three-dimensional numerical analyses that were carried out at the National Institute for Occupational Safety and Health (NIOSH), Pittsburgh Research Laboratory, to assess the stress and rock failure distribution for various geological and mine layout scenarios.

2.1 Horizontal Stress in Limestone Formations in the Eastern and Midwestern United States

Stress measurements and field observations have shown that the horizontal stresses in the limestone formations of the Eastern and Midwestern U.S. can be much higher than the overburden stress. Horizontal stresses in limestone formations have been measured in limestone mines [7] and in many of the area's coal mines [12]. Research has shown that the horizontal stress may be explained by the effect of plate tectonics [7, 13]. Tectonic loading is related to the movement of the North American plate as it is pushed away from the Mid-Atlantic ridge. A constant strain field of between 0.45 and 0.90 millistrains is associated with the tectonic loading, which induces higher horizontal stresses in the stiff limestone strata. The induced stress magnitude is not necessarily related to the cover depth for depths encountered in limestone mining operations, but rather to the stiffness of the strata. The typical elastic modulus of the limestones varies from 35 to 65 GPa. High horizontal stresses are not present in all the limestone formations because local features such as outcropping and folding may have relieved the stresses over geological time [8, 14]. Consequently, outcropping mines can have highly variable horizontal stress magnitudes which depend on the amount of relief that occurred and the distance from the outcrop.

A review of horizontal stress measurements in limestone and dolomite formations in the Eastern and Midwestern U.S. and Eastern Canada [13] shows that the maximum horizontal stress can vary between 4.1 MPa and 47.6 MPa up to depths of 300 m, shown in figure 1. Limited information is available at greater depths. A linear equation fitted to the maximum horizontal stress data produces the following:

$$\sigma_{h\max} \quad 0.041h + 9.51\,(MPa) \tag{1}$$

where: h is the depth in meters.

The orientation of the maximum horizontal stress is between N60°E and N90°E in 80% of the sites. This agrees with the regional tectonic stress orientation as indicated by the World Stress Map Project [15]. The magnitude of the minimum horizontal stress is approximately one half the maximum horizontal stress.

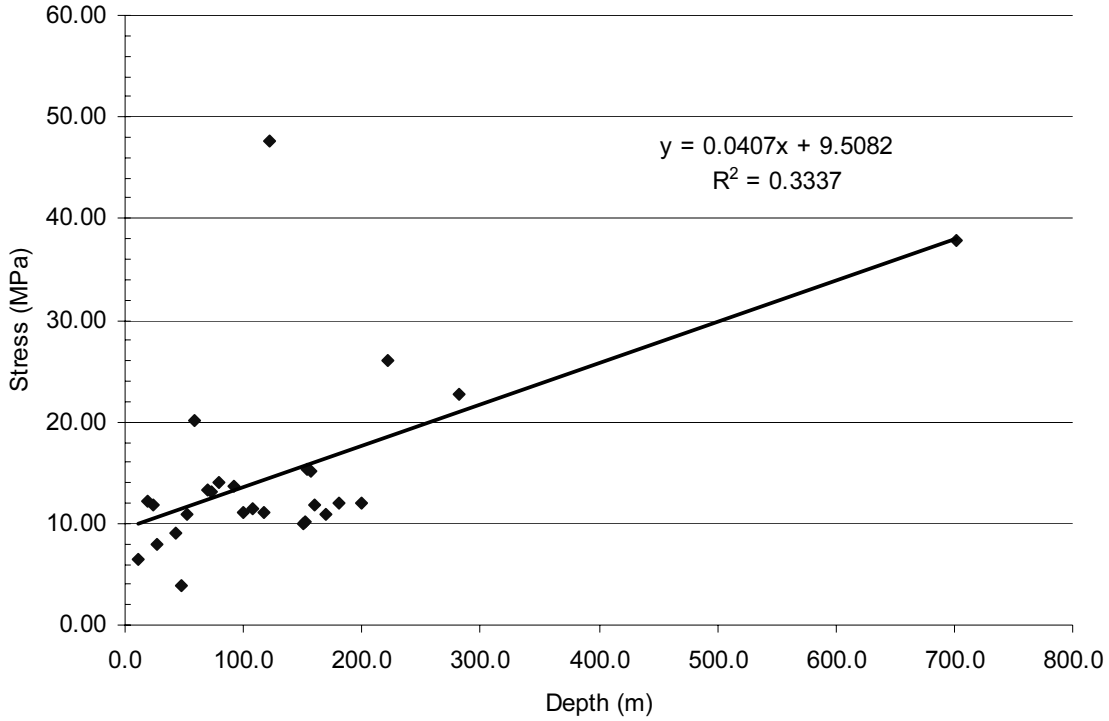

Figure 1. Maximum horizontal stress measurements in limestone and dolomite formations in the Eastern and Midwest U.S. and Eastern Canada, showing a fitted straight line and equation.

3.1 Roof Stability and Horizontal Stress Related Damage

3.1.1 Survey of Roof Stability in Limestone Mines

NIOSH researchers recently conducted a survey of roof conditions in 34 underground limestone mines to identify the factors contributing to roof instability [16]. The survey included conducting rock mass rating and laboratory strength testing of the intact limestone.

Rock mass rating (RMR) results showed that the limestone formations that are being mined fall in the range of 60-85 using the 1989 version of the classification system of Bieniawski [17]. The results of laboratory testing showed that 68% of average rock strength values for mine sites lie in the range of 120 MPa to 180 MPa. Joint frequency is on the order of 3 joints per meter and typically consist of two or more steeply dipping joint sets plus bedding. The steeper joints are typically rough and discontinuous while the bedding joints can be continuous over several tens of meters.

The survey further showed that about 46% of the mines regularly use roof reinforcement, while the remainder of the mines rely on the natural stability of the surrounding rock mass and may occasionally use rock reinforcement. Roof reinforcement was typically mechanical anchored or grouted rock bolts that are 1.8 to 2.4 m long.

It was found that horizontal stress contributed to roof damage at seven of the 34 mines visited during the survey. A review of the geological and mine layout parameters at these mines showed that they were not significantly different from the mines that did not experience horizontal stress related instability. For example, the depth of cover at the locations of stress related damage varied from 40 m up to 300 m, similar to that of the entire dataset. The average uniaxial compressive strength (UCS) of the limestone rocks at these mines was 188 MPa, which is not exceptional. The laboratory-determined elastic modulus of the rocks at the mines having horizontal stress stability problems was 63.8 GPa while it was 52.3 GPa at the remaining mines, which seems to indicate that high elastic modulus might be used as an indicator of potential roof stability problems. However, the data also showed that mines with higher elastic modulus values were not necessarily all subject to horizontal stress related instability. On the contrary, mines where the elastic modulus of the limestone was less than about 50 GPa were all free of horizontal stress related problems.

3.1.2 Observed Roof Damage Related to Horizontal Stress

Stress induced roof damage in limestone mines is similar in appearance to that seen in other bedded deposits such as coal mine roof strata [6, 12, 18]. Stress mapping techniques were used to identify the occurrence of horizontal stress related instability [18]. Various forms of roof damage were observed and are described below.

3.1.2.1 Roof Guttering

Horizontal stress related damage can manifest itself as guttering along the pillar-roof contact area [6, 19] as seen in figure 2. This is very similar to “cutter roof” seen in coal mines that are subject to high horizontal stresses. Once the roof has been damaged at the pillar contacts, the confining stresses are relieved and the immediate roof layers can fail. The failure can extend across the width of the excavation if it is not well supported. This type of failure has been observed in mines located in both inclined and flat lying limestone formations.

3.1.2.2 Beam Instability

The bedded rock in the roof of limestone mines can behave as individual beams or plates that can fail under gravity loading or as a result of the horizontal stress. In high horizontal stress conditions, buckling of the rock beds, stress fracturing and shearing of the beds can occur [5, 6, 16, 19]. Stepped roof and brows are signs of beam type failure. Mining under a thinly bedded roof usually requires regular support, such as patterned rock bolts, because the individual beds are unable to sustain their integrity over the span of the excavation. When mining under a more massive roof, the thicker roof beds may be naturally stable. However, when mining under an apparently massive roof, it becomes important to know the location of any weak bedding discontinuities so that thinner roof beds can be identified and appropriately supported.

Figure 2. Roof guttering at the pillar-roof contact.

3.1.2.3 Oval Shaped Falls

Another common manifestation of horizontal stress is large oval-shaped falls, with the long axis oriented approximately perpendicular to the major horizontal stress [6], as shown in figure 3. These falls typically initiate by failure of the lower roof bed and can progress upwards to form an arch-shaped cavity in the roof, as seen in figure 4. The mechanism of failure may be described as progressive shearing and buckling of the individual rock layers in the roof [9]. The failures are often preceded by excessive deflection of the roof beams which may be associated with microseismic emissions. Collapse of the roof beams is progressive in the vertical direction, with individual beds failing from the bottom up. These falls are often seen to initiate in the roof between two pillars.

3.1.2.4 Failure Propagation

Oval-shaped roof falls have been observed to gradually propagate in the lateral direction, perpendicular to the direction of the maximum horizontal stress. They can extend for several tens of meters, and can extend well over 100 m. Once an oval-shaped cavity is formed, the stress concentrations at the ends of the oval appear to cause further rock failure and growth of the failed zone in the lateral direction [6]. The propagation of the failure appears to be associated with relatively large roof deflections ahead of the failed cavity. An example of roof deflection and propagation of the roof fall cavity is shown in figure 5, after Iannacchione et al. [5]. In this case, the roof collapsed when the roof sag exceeded 5 cm at the indicated roof monitor location.

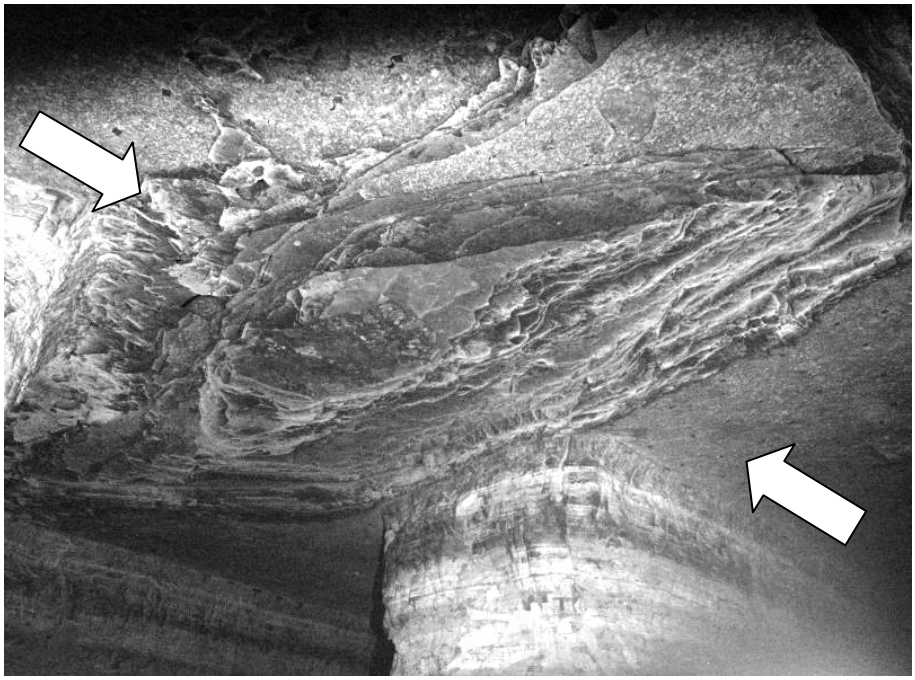

Figure 3. Horizontal stress induced roof failure that initiated between two pillars. Arrows show direction of maximum horizontal stress.

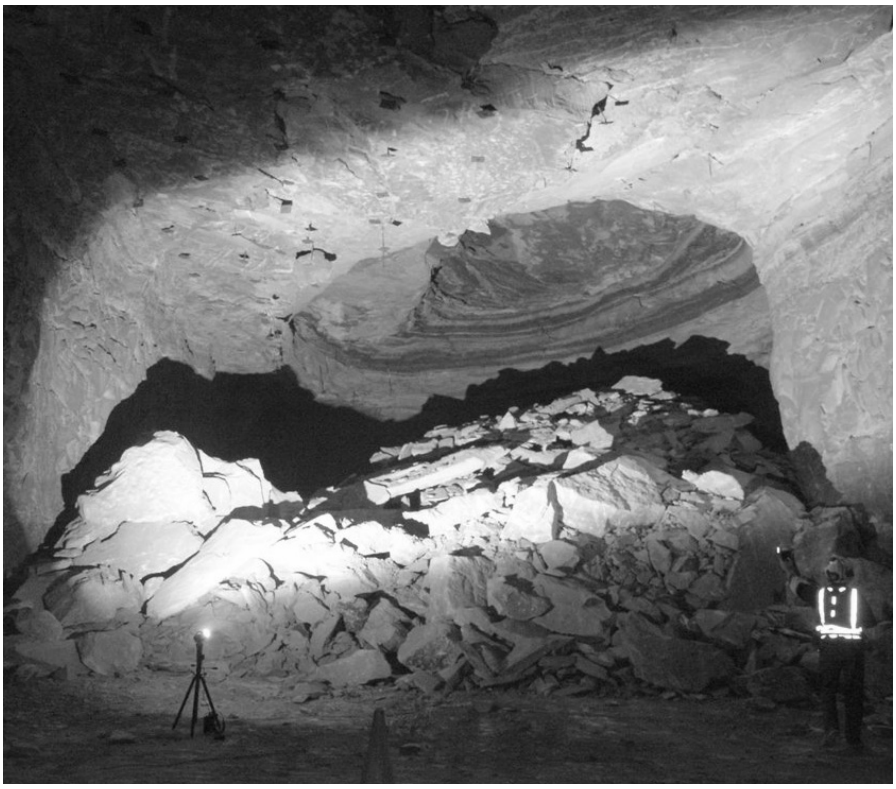

Figure 4. Large-oval shaped fall that has propagated upwards into weaker over lying strata in a limestone mine.

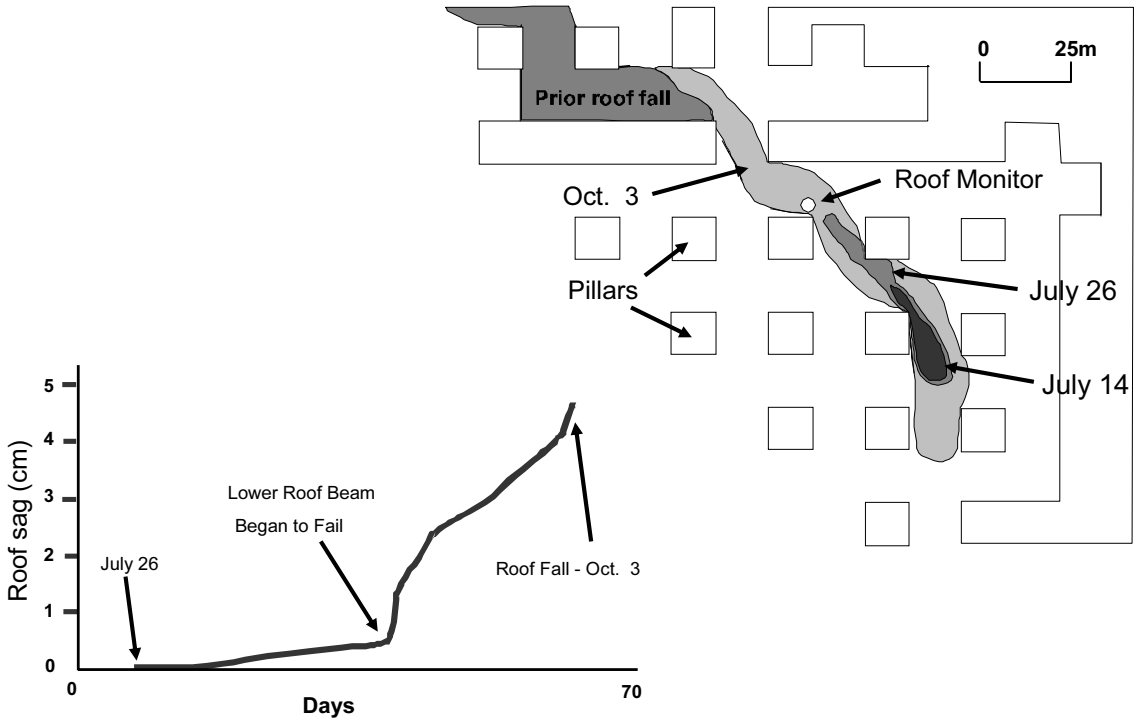

Figure 5. Progressive roof failure associated with high horizontal stress, showing roof sag measured at roof monitor ahead of the initial fall, after Iannacchione et al. [5].

3.2 Mitigation Alternatives

High horizontal stresses pre-exist mining and little can be done to completely avoid these stresses. Techniques that have been developed to alleviate the effects of horizontal stress in limestone mines include the selection of a stable roof line, favorable orientation of mine workings relative to the stress field, pillar layout modifications and installation of regular roof reinforcement. Re-orienting the excavations and modifications of mine layouts have been successful in improving roof conditions in several cases [8, 10, 11, 20]. The method includes re-orienting the mining layout so that the main direction of development is parallel to the direction of maximum horizontal stress and limiting the number of cross-cuts.

4.1 Analysis of Bedded Roof Stability in High Horizontal Stress Conditions

Roof bed stability in a three-dimensional mining layout can readily be assessed using numerical models, overcoming some of the limitations of analytical procedures such as classical beam theory or the ‘voussoir’ beam model [21, 22]. Numerical models allow the effect of initial horizontal stresses, complex excavation layouts, support elements and progressive rock failure to be simulated.

The FLAC 3D finite difference software [23] was used to assess roof stability for the typical stress conditions and mining dimensions that are found in U.S. limestone mines. For these analyses, the rock material was assumed to be elastic and bedding joints were

introduced in the models using the interface and ubiquitous joint logic in the FLAC 3D software. Various combinations of roof bed thickness and location of bedding discontinuities were modeled. The results were evaluated by reviewing the stress distributions and applying a rock failure criterion to the elastic stress results to identify potential zones of failure.

4.1.1 Model Design

A model was initially developed to evaluate the stress distribution and potential failure in the roof for various depths of cover, horizontal stress scenarios and various roof bed geometries. The model simulated an array of 14-m-wide rooms and pillars, which is representative of the excavations in limestone mining operations. Symmetry of the layout allowed only a quarter of a pillar and the adjacent rooms to be modeled. Interface elements were used to explicitly simulate roof bed discontinuities at various locations above the rooms.

A second, larger model, was set up to simulate an array of sixteen pillars and the surrounding rooms, which allowed various pillar configurations and loading conditions to be assessed. In order to avoid model edge effects, results were evaluated only in the central part of this model.

The models were set up to simulate workings at 100, 200, and 300-m depth. Only the 300-m depth results are presented here. The maximum horizontal stress at 300-m depth was set at 21.8 MPa, based on equation 1. The minimum horizontal stress was set equal to one half the maximum horizontal stress, while the vertical stress was 7.8 MPa, representing the cover loading.

The rock material properties were based on laboratory test results, the limestone having an elastic modulus of 50 GPa and Poisson's ratio of 0.2. The uniaxial compressive strength of the rock was set to 63 MPa, which is low relative to the typical strength values found in limestone mines. The rock strength was deliberately chosen to be low, so that the differences between the models would be more evident than when using a higher, more representative strength. The extent of failure is indicated by a failure index, which is calculated as the ratio of the rock strength to the maximum principal stress. A failure index of less than 1.0 can be interpreted as fractured rock that can potentially become unstable in the absence of support.

The rock failure criterion was based on a two-stage failure process consisting of brittle fracturing and frictional shearing [24, 25]. This failure process simulates the failure of hard brittle rocks in which extensional fractures develop parallel to the direction of the maximum principal stress at low confinement. At higher confinement values, the friction is mobilized in the rock, allowing the classical Coulomb failure criterion to be used. The brittle fracturing mode of failure can occur when the maximum principal stress is between 10% and 30% of the laboratory-scale uniaxial compressive strength [25, 26, 27] and has frequently been observed in limestone mine workings [26, 27, 28].

Bedding discontinuities were modeled with friction angle of 30° and cohesion of 1.0 MPa. The normal and shear stiffness of the bedding discontinuities were both set at 10 GPa.

4.1.2 Bedding Discontinuity Effects on Roof Stability

The first set of models was run to determine how the presence of bedding discontinuities affects the stress distribution and potential rock failure in the roof. The rock was assumed to be elastic and potential failure was identified by calculating the failure index. The intact rock was not permitted to fail and re-distribute the stress in these models. Some stress re-distribution did occur, however, when bedding discontinuities were modeled.

The results presented in figure 6 show the stress distribution in the immediate roof for a case without any bedding joints in the roof. It can be seen that the immediate roof is subject to elevated horizontal stresses in the rooms that are perpendicular to the major horizontal stress. The roof of the intersection area and rooms parallel to the major horizontal stress are subject to lower stresses. This indicates that if the stresses are sufficiently high to cause compressive failure of the roof, the area between pillars is more likely to fail than the intersections, which is consistent with observations.

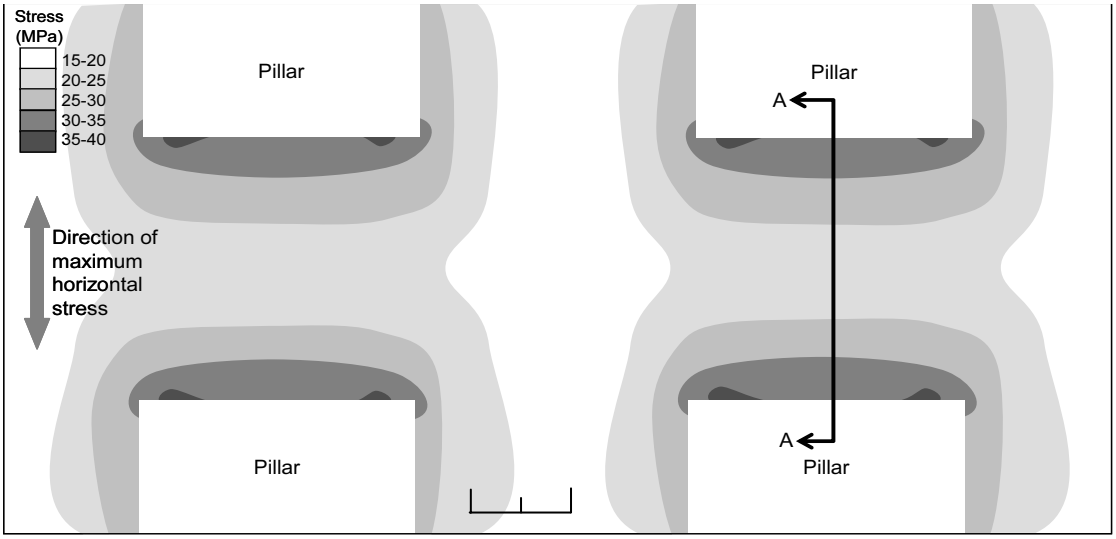

Figure 6. Plan view of numerical model results showing contours of horizontal stress 1 m above the roof of a room and pillar layout located at 300 m depth subject to a maximum horizontal stress magnitude of 21.8 MPa.

The failure index results in figure 7a show that, in the absence of bedding discontinuities, rock failure potential is a maximum at the pillar-roof contact and can extend over the room to form an arch of potential failure up to about 3 m above the roof line. If a single bedding discontinuity is introduced 1 m above the roof line, see figure 7b, the stresses are re-distributed by the presence of the discontinuity. A reduction occurs in the horizontal stress in the 1-m-thick roof beam as it deflects downwards and

some slip occurs along the bedding discontinuities. Separation of up to 2 mm occurs across the bedding discontinuity near the center of the room. The beam deflection causes an increase in horizontal stress as well as a reduction in confining stress in the overlying roof, which causes the potential rock failure to extend to 4 m above the roof line.

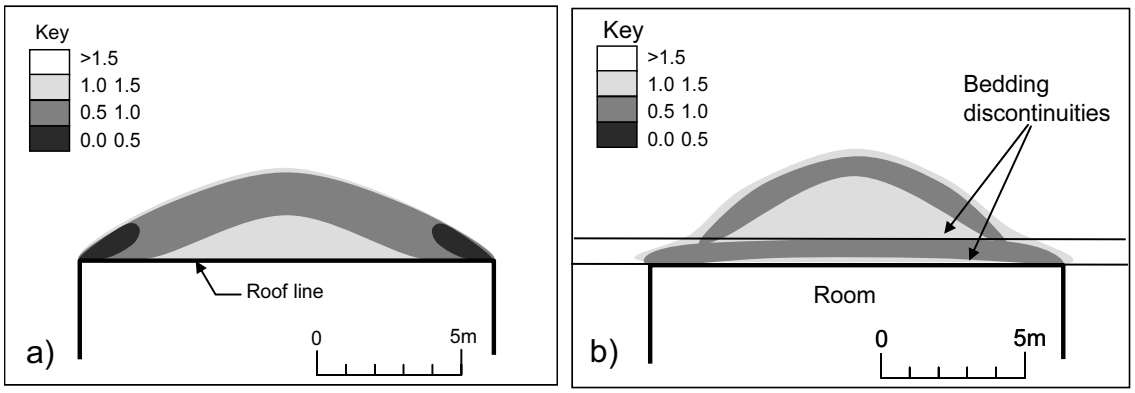

Figure 7. Vertical section along A-A in figure 5 showing rock failure index values (a) without bedding discontinuities and (b) with a bedding discontinuity 1 m above the roof line.

A third model was set up in which three bedding discontinuities 1 m apart were introduced above the roof line, shown in figure 8a. The potential failure now extends up to 5 m above the roof line as beam deflection and stress redistribution continues further into the roof.

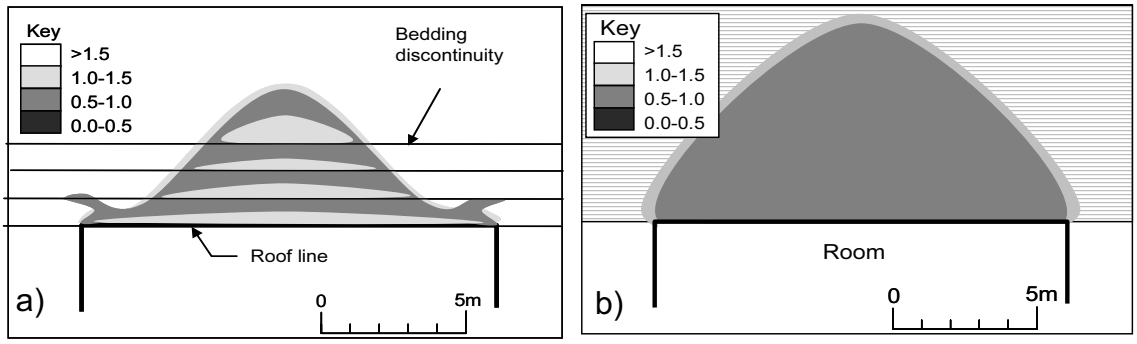

Figure 8. Vertical section along A-A in figure 5 showing rock failure index values (a) with three 1-m-thick bedding discontinuities in the roof and (b) thinly laminated roof.

In the final case the roof is modeled as a thinly bedded rock using the ubiquitous joint logic in FLAC 3D. This assumed that each element in the model contains horizontal planes of weakness that can shear. The strength of these ubiquitous weaknesses was set equal to that of the bedding discontinuities described above. The stability index results are shown in figure 8b which showed the extent of potential failure is much greater, now extending about 10 m above the roof line. Inspection of the results showed that slip along the roof beds allowed more roof deflection to occur which reduced the confinement in the roof.

4.1.3 Assessment of Room and Pillar Layout Alternatives

The larger FLAC 3D model was first used to compare potential roof failure in a regular room and pillar layout using square pillars. A second assessment was made of a layout containing rectangular, offset pillars.

For these models, it was assumed that a 5-m-thick limestone layer was present in the roof of the excavations. Failure of the roof was again determined using a relatively low strength of the limestone to highlight the differences between the layouts. Initial rock failure was determined in the models from the elastic stress distribution. Potential failure growth was determined by invoking the Coulomb-based strain softening logic in FLAC 3D. A special function was developed using the internal programming language of FLAC 3D to simulate the brittle/shearing failure mode described earlier. Using this approach, stresses are re-distributed in response to the initial failure which causes further failure to occur. The models were allowed to run until no more failure growth occurred.

4.1.3.1 Assessment of a Square Pillar Layout

Figure 9 shows the initial failure and failure growth in the roof for a layout of square pillars that is (a) aligned with the direction of maximum horizontal stress and (b) the stress is rotated through 45°. These results show that for the first case, failure is likely to initiate between pillars and will grow in the direction perpendicular to the maximum horizontal stress, similar to the behavior observed in limestone mines. A practical issue with this type of failure is that once failure starts, it is free to extend laterally across the width of the mine until a solid abutment or barrier pillar is encountered.

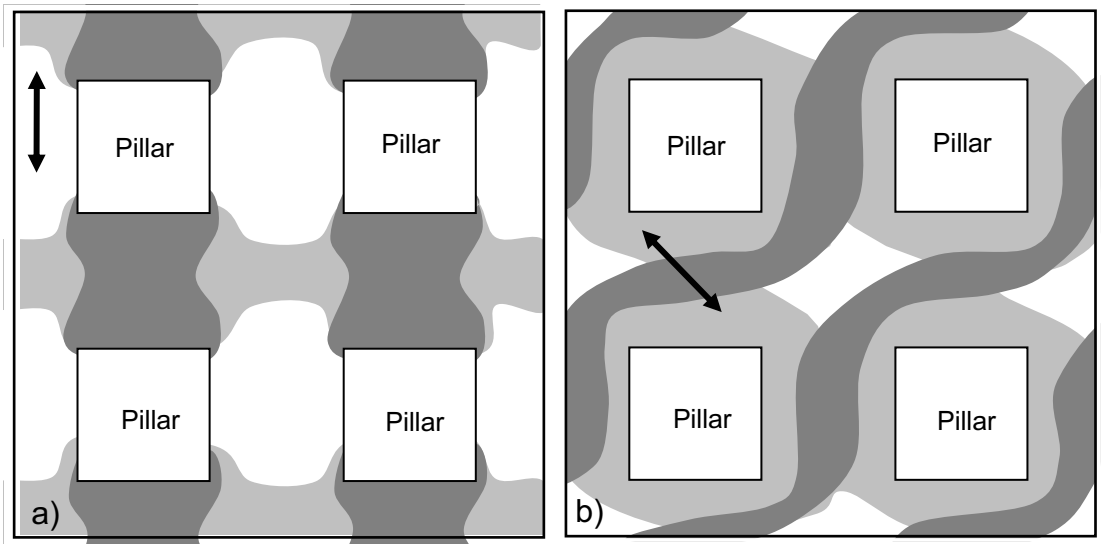

Figure 9. Plan view showing effect of a change in the orientation of the maximum horizontal stress potential roof failure in a room and pillar layout consisting of square pillars. Darker shading indicates initial failure and lighter shading indicates potential failure growth. The arrow indicates the direction of maximum horizontal stress.

The results for the 45° case show that roof failure is likely to snake through the pillars, similar to the failure seen in the field study presented in figure 5. Again, this type of failure can continue to extend laterally until a barrier or abutment is encountered. The model showed that ultimate roof failure can encircle the pillars, which was observed in one location at the mine site as shown in figure 5.

4.1.3.2 Assessment of a Rectangular Pillar Layout

The practice of aligning pillars and heading development parallel to the direction of maximum horizontal stress was simulated to determine whether the models would reflect the improved stability of this type of layout. The model was set up to simulate rooms and pillars that were the same width as those shown in figure 9, except that the pillar length in the direction parallel to the maximum horizontal stress was doubled. In addition, the crosscuts were offset, a common practice in the limestone mines, so that the lateral growth of roof failure is restricted. The results shown in figure 10a, presents a case where the crosscuts are located opposite the center of the adjacent pillar, that is, the offset is a maximum. It can be seen that potential failure initiation is very similar to that shown in figure 9a for the square pillar layout. However, failure growth is restricted to the vicinity of the crosscut. Should the failure extend across the adjacent rooms, it will encounter the adjacent pillar, which will halt its growth. Figure 10b shows a case where the cross-cut offset has been reduced. Here, it can be seen that the initial failure is again similar to the previous case, but the failure growth cuts across the headings into the adjacent cross-cuts, resulting in the potential for a continuous band of failures across the width of the mined area.

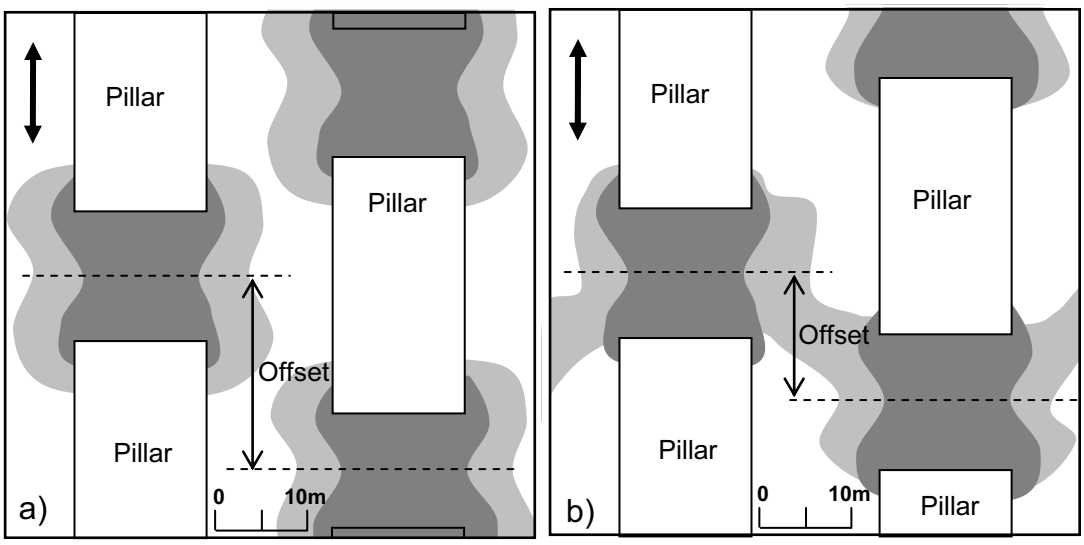

Figure 10. Plan view showing effect of a change in the pillar offset on potential roof failure in a room and pillar layout consisting of rectangular pillars. Darker shading indicates initial failure and lighter shading indicates potential failure growth. The arrow indicates the direction of maximum horizontal stress.

Operating limestone mines that have adopted a rectangular pillar layout aligned with the maximum horizontal stress typically reduce the cross-cut width to reduce the exposure to potentially unstable roof. In some cases, the cross-cut roof is lowered and arched so that it is not exposed to the horizontal stresses in the main roof.

5.1 Conclusions

This review and study of horizontal stress related stability issues in U.S. limestone mines has shown that:

a) Horizontal stresses in limestone formations in the Eastern and Midwestern United States are the result of plate tectonics and can result in roof damage in limestone mines.
b) About 20% of the mines surveyed by NIOSH researchers experienced horizontal stress related roof damage.
c) Large oval shaped stress induced rock falls represent a significant safety and operational hazard. These falls can extend for many tens of meters across a mined area, blocking access to mine workings beyond.
d) Numerical analyses using a two-stage brittle/shearing failure criterion appears to capture the essence of roof instability in hard and brittle limestone formations.
e) The model studies showed that bedding discontinuities in the immediate roof can exacerbate the depth and extent of rock failure in the roof. Roof stability is further degraded by increased deflection and separation of the bedded roof.
f) The models and mine experience both show that there is great advantage in aligning the pillar layout parallel to the direction of maximum horizontal stress and offsetting crosscuts so that lateral growth of roof failures is restricted.
g) The numerical modeling approach presented in this paper can be used to assist in limestone mine layout design when confronted with horizontal stress related stability problems.

Disclaimer

The findings and conclusions in this report have not been formally disseminated by the National Institute for Occupational Safety and Health and should not be construed to represent any agency determination or policy.

References

1. Mine Safety and Health Administration (2007). Website, http://www.msha.gov, accessed October 2007.

2. Hasenfus, G. J. and Su, D. W. H. (2006). Horizontal stress and coal mines: twenty five years of experience and perspective. Proceedings, 25th International Conference on Ground Control in Mining, Morgantown, WV, pp. 256-267.

3. Parker, J. (1966). Mining in a lateral stress field at White Pine, Trans. Canadian Inst. Min. Metal. V LXIX pp. 375-383.

4. Emery, C. L. (1964). In Situ Measurements Applied to Mine Design. Proceedings, 6th Symposium on Rock Mechanics, Rolla, MO, pp 218-230.

5. Iannacchione, A. T., Dolinar, D. R., Prosser, L. J., Marshall, T. E., Oyler, D. C., and Compton, C. S. (1998). Controlling Roof Beam Failures from High Horizontal Stresses in Underground Stone Mines. Proceedings, 17th International Conference on Ground Control in Mining, Morgantown, WV, pp. 102-112.

6. Iannacchione, A. T., Marshall, T. E., and Prosser, L. J. (2001). Failure Characteristics of Roof Falls at an Underground Stone Mine in Southwestern Pennsylvania. Proceedings, 20th International Conference on Ground Control in Mining, Morgantown, WV, pp. 119-125.

7. Iannacchione, A. T., Dolinar, D. R., and Mucho, T. P. (2002). High Stress Mining Under Shallow Overburden in Underground U.S. Stone Mines. Proceedings, First International Seminar on Deep and High-Stress Mining, Nedlands, Australia: Australian Centre for Geomechanics, section 32, pp. 1-11.

8. Iannacchione, A. T., Marshall, T. E., Burke, L., Melville, R., and Litsenberger, J. (2003). Safer Mine Layouts for Underground Stone Mines Subjected to Excessive Levels of Horizontal Stress. Min Eng 55(4):25-31.

9. Iannacchione, A. T., Esterhuizen, G. S., Bajpayee, T. S., Swanson, P. L., and Chapman, M. C. (2005). Characteristics of Mining-Induced Seismicity Associated with Roof Falls and Roof Caving Events. Proceedings, 40th U.S. Rock Mechanics Symposium, Anchorage, Alaska, paper 05-678.

10. McGunegle, B. F. and Adu-Acheampong, A. (2005). Stability Assessment of an Underground Limestone Mine A Case Study. Proceedings, 40th U.S. Rock Mechanics Symposium, Anchorage, Alaska, paper 05-872.

11. Kuhnhein, G. and Ramer, R. (2004). The Influence of Horizontal Stress on Pillar Design and Mine Layout at Two Underground Limestone Mines. Proceedings, 23rd International Conference on Ground Control in Mining. Morgantown, WV, pp. 311-319.

12. Mark, C. and Mucho, T. P. (1994) Longwall Mine Design for Control of Horizontal Stress. U.S. Bureau of Mines Special Publication 01- 94, New Technology for Longwall Ground Control, pp. 53-76.

13. Dolinar, D. (2003). Variation of Horizontal Stresses and Strains in Mines in Bedded Deposits in the Eastern and Midwestern United States. Proceedings, 22nd International Conference on Ground Control in Mining, Morgantown, WV, pp. 178-185.

14. Iannacchione, A. T. and Coyle, P. R. (2002). An Examination of the Loyalhanna Limestone's Structural Features and their Impact on Mining and Ground Control

Practices. Proceedings, 21st International Conference on Ground Control in Mining, Morgantown, WV, pp. 218-227.

15. World Stress Map Project (2007). Website http://www-wsm.physik.uni-karlsruhe.de, accessed April 2007.

16. Esterhuizen, G. S., Dolinar, D. R., Ellenberger, J. L. Prosser, L. J. and Iannacchione, A. T. (2007). Roof Stability Issues in Underground Limestone Mines in the United States. Proceedings, 26th International Ground Control Conference, Morgantown, WV, pp. 320-327.

17. Bieniawski, Z. T. (1989). Engineering Rock Mass Classifications. New York: Wiley.

18. Mucho, T. P. and Mark, C. (1994). Determining Horizontal Stress Direction Using the Stress Mapping Technique. Proceedings, 13th Conference on Ground Control in Mining, Morgantown, WV, pp. 277-289.

19. Esterhuizen, G. S. and Iannacchione, A.T. (2004). Investigation of Pillar-Roof Contact Failure in Northern Appalachian Stone Mine Workings. Proceedings, 23rd International Conference on Ground Control in Mining, Morgantown, WV, pp. 320-326.

20. Parker, J. (1973). How to Design Better Mine Openings: Practical Rock Mechanics for Miners. Engineering and Mining Journal, Part 5, December, pp. 76-80.

21. Brady, B. H. G. and Brown, E. T. (1985). Rock Mechanics for Underground Mining. George Allen and Unwin, London, 527 pp.

22. Diederichs, M. S. and Kaiser P. K. (1999). Stability of Large Excavations in Laminated Hard Rock Masses: The Voussoir Analogue Revisited. International Journal of Rock Mechanics and Mining Sciences 36:97-117.

23. Anon (2006) FLAC 3D, Fast Lagrangian Analysis of Continua, User's Manual Version 3.1. Itasca Consulting Group, Minneapolis, Minnesota.

24. Diederichs, M. S. (2002). Stress Induced Damage Accumulation and Implications for Hard Rock Engineering. NARMS-TAC 2002, Hammah Et Al. (Eds), University of Toronto, pp. 3-12.

25. Kaiser, P. K., Diederichs, M. S., Martin, D. C. and Steiner, W. (2000). Underground Works in Hard Rock Tunneling and Mining. Keynote Lecture, Geoeng2000, Melbourne, Australia, Technomic Publishing Co., pp. 841-926.

26. Esterhuizen, G. S. (2006). Evaluation of the Strength of Slender Pillars. Trans Soc Min Metal Explor 320:69-76

27. Alber, M. and Heiland, J. (2001a). Investigation of a Limestone Pillar Failure Part 1: Geology, Laboratory Testing and Numerical Modeling. Rock Mechanics and Rock Engineering 34(3):167-186.

28. Bawden, W. F. and McCreath, D. R. (1979). Geotechnical Study of an Abandoned Limestone Mine for Crude Oil Storage. Can, Geotech. J. 16:577-590.

29. Stacey, T. R. and Yathavan, K. (2003). Examples of Fracturing of Rock at Very Low Stress Levels. ISRM 2003 Technology Roadmap for Rock Mechanics, S. Afr. Inst. Min. Metall., pp. 1155-1159.